Journal of
Synchrotron Radiation

ISSN 0909-0495

addenda and errata

X-ray spectroscopic approaches to the investigation and characterization of photochemical processes. Erratum

Pierre Kennepohl,[a]* Erik C. Wasinger[b] and Serena DeBeer George[c]

[a]The University of British Columbia, Department of Chemistry, Vancouver, BC, Canada V6T 1Z1, [b]California State University, Chico, Department of Chemistry, Chico, CA 95929, USA, and [c]Stanford Synchrotron Radiation Laboratory, SLAC, Stanford University, Stanford, CA 94309, USA. E-mail: pierre@chem.ubc.ca

An error in the paper by Kennepohl *et al.* [(2009), *J. Synchrotron Rad.* **16**, 484–488] is corrected.

In the paper by Kennepohl *et al.* (2009), an important statement in the Acknowledgements section was omitted. The following text should have been included:

We wish to thank Professor Jeffrey Rack and Dr Aaron Rachford for the sample of $[Ru(tpy)(bpy)(DMSO)](OSO_2CF_3)_2$ used in this study and for helpful discussions.

References

Kennepohl, P., Wasinger, E. C. & DeBeer George, S. (2009). *J. Synchrotron Rad.* **16**, 484–488.

  doi:10.1107/S0909049509048237

Journal of
Synchrotron Radiation

ISSN 0909-0495

Received 18 September 2008
Accepted 5 June 2009

X-ray spectroscopic approaches to the investigation and characterization of photochemical processes

Pierre Kennepohl,[a]* Erik C. Wasinger[b] and Serena DeBeer George[c]

[a]The University of British Columbia, Department of Chemistry, Vancouver, BC, Canada V6T 1Z1, [b]California State University, Chico, Department of Chemistry, Chico, CA 95929, USA, and [c]Stanford Synchrotron Radiation Laboratory, SLAC, Stanford University, Stanford, CA 94309, USA. E-mail: pierre@chem.ubc.ca

Despite a wealth of studies exemplifying the utility of the 2–5 keV X-ray range in speciation and electronic structure elucidation, the exploitation of this energy regime for the study of photochemical processes has not been forthcoming. Herein, a new endstation set-up for *in situ* photochemical soft X-ray spectroscopy in the 2–5 keV energy region at the Stanford Synchrotron Radiation Lightsource is described for continuous photolysis under anaerobic conditions at both cryogenic and ambient temperatures. Representative examples of this approach are used to demonstrate the potential information content in several fields of study, including organometallic chemistry, biochemistry and materials chemistry.

Keywords: X-ray absorption spectroscopy; XAS; photochemistry; *in situ* photolysis.

1. Introduction

The development and expansion of the use of soft X-ray methods for the evaluation and characterization of electronic structure has allowed for new insights in diverse areas of chemistry. In particular, beamline 6-2 at the Stanford Synchrotron Radiation Lightsource (SSRL) has provided researchers with many opportunities to explore a wide range of problems in the 2–5 keV energy region, a region that allows for the investigation of elements that cannot be easily accessed by other methods. In the near future, such experiments including all capabilities described herein will move to SSRL BL 4-3. Specifically, the use of sulfur and chlorine *K*-edge X-ray absorption spectroscopy (XAS) for speciation as well as more detailed investigations has been of particular note (Delgado-Jaime *et al.*, 2006; Dey *et al.*, 2007; DeBeer George *et al.*, 2006; Leung *et al.*, 2008; Martin-Diaconescu & Kennepohl, 2007; Ray *et al.*, 2007; Tenderholt *et al.*, 2008). In addition, this energy region is appropriate for second-row transition metal *L*-edges, which are emerging as important spectroscopic probes in homogeneous catalysis and in other areas. Such studies have widened the impact of this energy region and have led to the use of XAS in emerging areas of interest.

An area which has thus far been poorly explored is the application of soft X-ray XAS for the study of photochemical processes. We report herein a new endstation set-up for soft X-ray spectroscopy at SSRL which allows for continuous photolysis under anaerobic conditions at both cryogenic and ambient temperatures. We provide several representative examples that demonstrate the potential information content of this approach.

2. Methodology

For experiments in the 2–5 keV range, the very short path length of X-rays in air requires enclosure of the entire flight path in a helium atmosphere. The set-up at SSRL beamline 6-2 utilizes computer-controlled JJ X-ray slits in a KF-40 flanged vacuum- and helium-compatible configuration as shown in Fig. 1. The slits are coupled to the beamline exit port and the sample box space using vacuum-compatible bellows, which reduce helium leakage to a minimum. The incident beam intensity is measured using a helium-filled ionization chamber that is isolated from the sample space by a 6 µm polypropylene window. Downstream of the slits, a five-way cross houses a motorized linear motion feedthrough, which has both a fluorescent screen (which may be viewed using a camera outside of the five-way cross) for sample alignment and a reference calibrant for external calibration (the fluorescence signal of which is measured using an IRD AXUV-300 photodiode), see Fig. 1(*c*). This is followed by an additional set of bellows, which allows for a flexible configuration for different modular set-ups. In order to enable *in situ* photochemistry, the downstream bellows is connected to an inert atmosphere glove bag, which is purged with helium. An Alpha Omega Series 2000 oxygen sensor, with an accuracy of 0.005% in its lowest range of operation (0–0.5% oxygen), is used to monitor the quality of the helium purge. The sample is positioned at 45° relative to the incident beam and a Lytle detector (at 90° to the incident beam) is used for fluorescence measurements. For *in situ* photochemistry, experiments are performed in combination with a Ushio 75 W xenon arc lamp, as shown in Fig. 1(*b*). This set-up has also been used in combination with

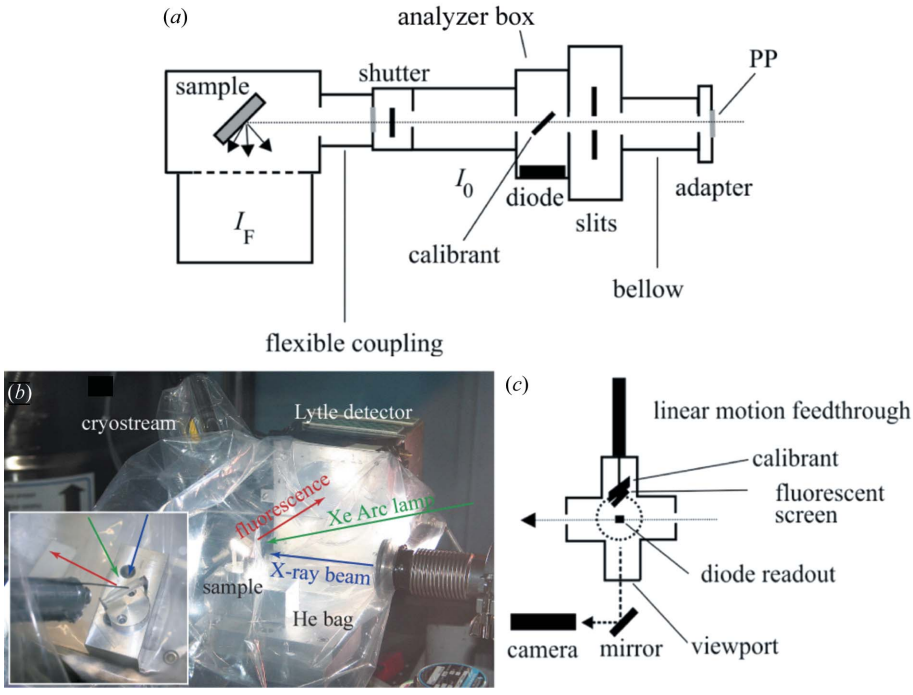

Figure 1
(*a*) Top view of the 2–5 keV set-up for BL6-2. (*b*) Photograph of a sample compartment during photolysis experiment using a 75 W Xe arc lamp; the inset shows the top view of a sample holder, and arrows qualitatively indicate photon beam paths during the experiment. (*c*) Side view of the analyzer box. Abbreviations: I_0, incident beam intensity; I_F, fluorescence intensity; PP, polypropylene window.

an open-flow liquid-helium cooler from Cryo Industries (HFC-1645 LHE-Cryocool). This allows data to be obtained at ~50 K without absorption owing to cryostat windowing material (which is significant at these energies). Active heating or thermal isolation of the Lytle detector is required when using the cryo-cooler.

Time-resolved data acquisition can be achieved in two different modes. Data are generally collected in a rapid scanning mode, where the edge region is scanned with short dwell times and data acquisition times (~0.1–0.2 s point^{-1}) to achieve a scan-to-scan time resolution of 2–10 min depending on the energy range used in the data acquisition. We have noted that increasing scan rates in this way does not significantly affect data integrity although signal/noise does deteriorate on lowering from 0.2 s point^{-1} to 0.1 s point^{-1}; this effect is negligible for solid samples where signal intensity is very strong. For faster data acquisition (*i.e.* to bypass monochromator repositioning, the slowest step in energy scanning), continuous data acquisition at a fixed photon energy is limited by detector readout rates, allowing for subsecond data acquisition using a Lytle detector.

3. Examples

3.1. Photochemical ligand isomerization of Ru complexes

Owing to their potential as molecular sensors and as optical molecular information storage devices, the development of photoswitchable bistable molecules is of considerable interest (Carducci *et al.*, 1997; Imlau, Haussiihl *et al.*, 1999; Imlau, Woike *et al.*, 1999). For photonic devices, the efficient conversion of light to usable potential energy is required. Bistable photochromic complexes are one class of photonic devices which depend on irradiation in the visible or ultraviolet range to trigger the conversion from one stable molecular form to a second stable molecular form. This photo-induced linkage isomerization has been observed and studied in many transition metal complexes containing ligands such as NO^+, NO_2^-, N_2, SO_2 and dimethylsulfoxide (DMSO) (Coppens *et al.*, 2002; Fomitchev *et al.*, 2000; Hortala *et al.*, 2003). A series of ruthenium complexes, $[Ru(tpy)(L)(DMSO)]^{2+}$ (tpy = 2,2′:6′,2″-terpyridine), utilizing the DMSO ligand to effect and exhibit bistability has been developed (Rachford *et al.*, 2005, 2006, 2007; Rachford & Rack, 2006; Rack & Mockus, 2003; Rack *et al.*, 2003). Interestingly, the ability of the DMSO ligand to switch between S-bound and O-bound coordination to ruthenium is highly dependent upon the bidentate auxiliary ligand (L) on the central ruthenium ion.

As part of a larger study, we have investigated the linkage isomerization of the solid [Ru(tpy)(bpy)(DMSO)]-$(OSO_2CF_3)_2$ (bpy = 2,2′-bipyridine) (1) complex using the experimental set-up shown in Fig. 1. Photochemically induced changes in the S *K*-edge XAS spectrum of (1) were observed as a function of time. Prior to visible light irradiation, the sample exhibits no low-energy absorption features in the S *K*-edge XAS spectrum in the 2465–2475 eV range (see Fig. 2). X-ray photoreduction or other photodamage is not observed over time under ambient lighting conditions. Upon photolysis, a new low-energy feature begins to appear at ~2475 eV and continues to grow during extended photolysis. The kinetic data show clear isosbestic points, suggesting clean photochemical conversion. The formation of an intense low-energy feature in the spectrum may originate from a low-lying π^* orbital with significant S 3*p* character, which is consistent with significant ligand reorganization at DMSO. A detailed analysis of the spectroscopic features and their kinetic profiles is underway.

3.2. Photodegradation olefin metathesis catalysts

The use of olefin metathesis as a simple and efficient approach to the creation and modification of carbon–carbon double bonds has exploded in the last ten years (Chauvin, 2006; Connon & Blechert, 2003; Furstner, 2000; Grubbs, 2004, 2006; Nicolaou *et al.*, 2005; Schrock, 2006). A major reason for this has been the development of robust and highly active

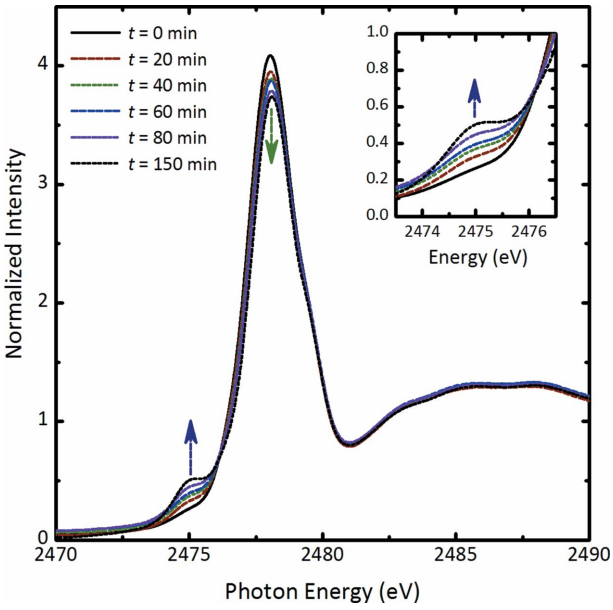

Figure 2
Direct photolysis of [Ru(tpy)(bpy)(DMSO)]$(OSO_2CF_3)_2$ followed by S *K*-edge XAS. The new feature attributed to O-bound DMSO is shown in the inset.

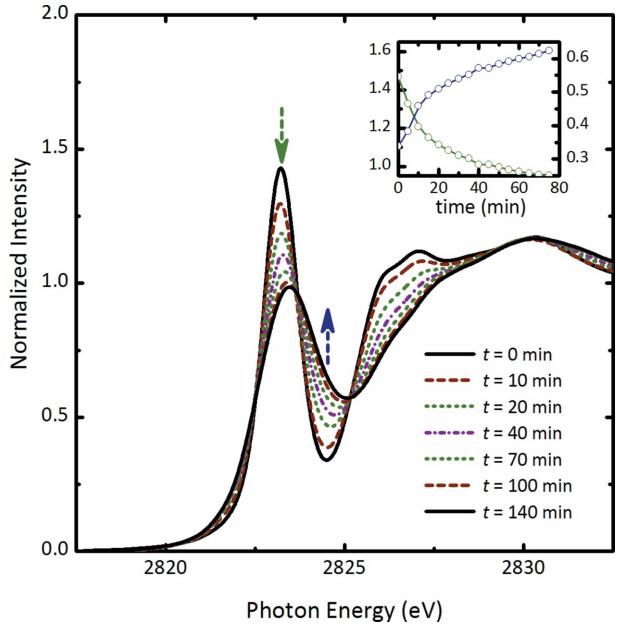

Figure 3
Direct photolysis of Grubbs' first-generation catalyst followed by Cl *K*-edge XAS. The inset provides kinetic profiles at 2823 eV (green) and 2824.5 eV (blue).

ruthenium carbene-based catalysts with high functional group tolerance, allowing their use in a wide variety of applications. However, there are several issues that remain unresolved in both the fundamental chemistry of these catalysts and their application in industrial applications. For example, the effects of potential photochemical degradation pathways of such catalysts (and their precursors) at all stages of processing are a relatively unexplored area (Kunkely & Vogler, 2001).

Within a larger effort to understand the electronic structure and reactivity of such species (Delgado-Jaime *et al.*, 2006; Getty *et al.*, 2007, 2008), we have explored the photochemical decomposition of Grubbs' first-generation catalyst by XAS as a means of evaluating the possible degradation pathways that may occur. We have obtained Cl *K*-edge XAS data during photoirradiation as shown in Fig. 3. Decomposition is slow but clearly observable in the Cl *K*-edge data with a dramatic change in the pre-edge feature, indicating an important change in the nature of the chloride ligand. The pre-feature feature in the pre-catalyst is a sharp feature that reflects the covalency of the Ru—Cl bonds through interactions of the valence Cl 3*p* orbitals and one of the empty Ru $4d_{\sigma*}$ orbitals. Upon photoirradiation the pre-edge splits into multiple features resulting in a broadening of the pre-edge region; however, the total intensity of the pre-edge increases during this process. Concomitantly, there is a small but reproducible change in the energy of the ionization edge position to higher energy, implying oxidation of the Cl^- ligand.

Although further study is required to explore the specifics of this reaction, the data are consistent with photodecomposition of the mononuclear ruthenium carbenes to form dimers (or larger species) with bridging chloride ligands such as those which have been isolated by others (Amoroso *et al.*, 2001, 2002; Hong *et al.*, 2004).

3.3. Photooxidation/reduction of amino acids

Amino acids and peptides are used extensively as food additives and increasingly as drugs. However, the long-term stability of these species and the possible products of photochemical decomposition have not been fully explored. It has been observed that oxidation of the natural amino acid methionine ($R = -CH_2SCH_3$) is an important factor in the stability of proteins and peptides, which can play an important role in human health (Cherian & Abraham, 1995; Glaser *et al.*, 2005; Requena *et al.*, 2004; Jacob *et al.*, 2003; Kadlcik *et al.*, 2006; Kishita *et al.*, 2005; Lam *et al.*, 1997). For this reason we feel it important to evaluate the reactivity of such species towards photodecomposition (Karunakaran-Datt & Kennepohl, 2009).

Anaerobic exposure of solid N-acetylated methionine (N-AcMet) to a Xe arc lamp under ambient temperatures indicates only subtle changes in the S *K*-edge XAS spectrum for 60 min (see Fig. 4*b*). Importantly, a small yet reproducible feature appears in the pre-edge region (see supplementary material[1]). Such features have been previously attributed to the formation of sulfur-centred radicals (Martin-Diaconescu & Kennepohl, 2007). This appearance of a signal in the electron paramagnetic resonance spectrum upon photoirradiation further implies the formation of a sulfur-centred free radical but only in small amounts and without further reactivity. By contrast, aerobic photoinitiation of N-AcMet (Fig. 4*a*) leads to rapid oxidation to the sulfoxide (~2477 eV) and sulfone (~2481 eV) (Karunakaran-Datt & Kennepohl, 2009; Frank *et*

[1] Supplementary data for this paper are available from the IUCr electronic archives (Reference: WA5008). Services for accessing these data are described at the back of the journal.

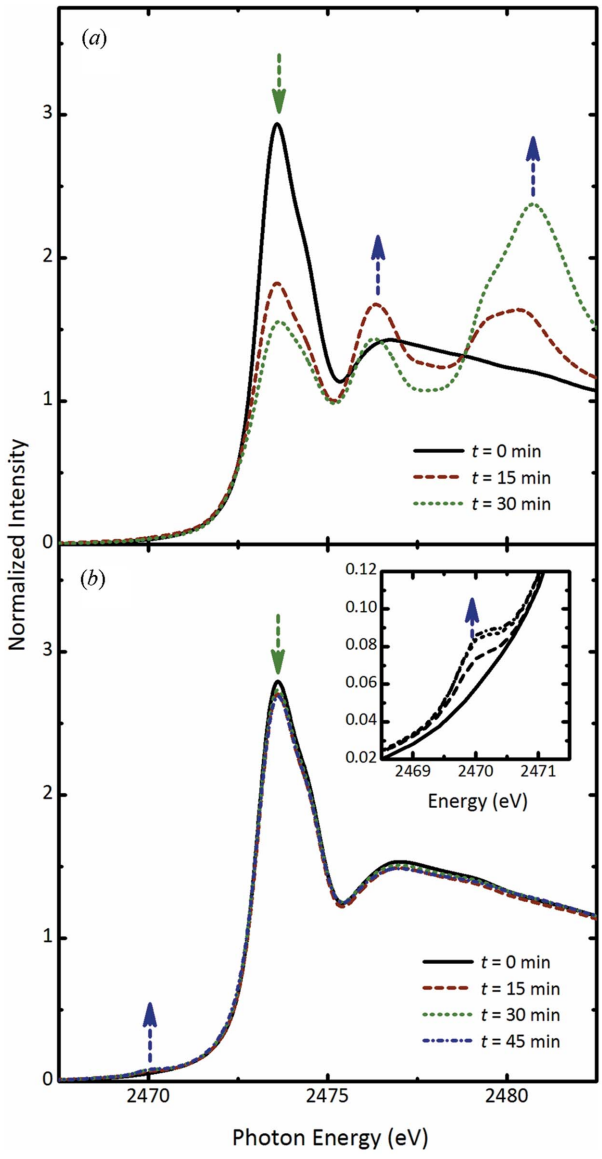

Figure 4
Photochemistry of methionine in the presence (*a*) and absence (*b*) of dioxygen. The inset gives a more detailed look at the formation of a low-energy pre-edge feature during photolysis.

al., 2006; Pickering *et al.*, 1998). These results and the related photochemistry of the oxidized forms of methionine have now been studied extensively and provide new insights into the redox chemistry of this natural amino acid.

4. Conclusions

A new endstation assembly has been developed and implemented at beamline 6-2 (and recently implemented at beamline 4-3) at the Stanford Synchrotron Radiation Lightsource allowing for temperature-controlled photolysis experiments with concomitant XAS data acquisition with resolution ranging from seconds to hours. The availability of this new experimental station allows for direct evaluation of photochemical processes using the power of element-specific synchrotron techniques.

Portions of this research were carried out at SSRL, a national user facility operated by Stanford University on behalf of the US DOE-BES. The SSRL Structural Molecular Biology Program is supported by DOE, Office of Biological and Environmental Research, and by the NIH, National Center for Research Resources, Biomedical Technology Program. This publication was made possible by Grant No. 5 P41 RR001209 from the National Center for Research Resources (NCRR), a component of the National Institutes of Health (NIH). Its contents are solely the responsibility of the authors and do not necessarily represent the official view of NCRR or NIH. Special thanks to Drs Matthew Latimer and Erik Nelson (SSRL) for assistance with the liquid-helium cryostream assembly and technical assistance.

References

Amoroso, D., Yap, G. P. A. & Fogg, D. E. (2001). *Can. J. Chem.* **79**, 958–963.
Amoroso, D., Yap, G. P. A. & Fogg, D. E. (2002). *Organometallics*, **21**, 3335–3343.
Carducci, M. D., Presspich, M. R. & Coppens, P. (1997). *J. Am. Chem. Soc.* **119**, 2669–2678.
Chauvin, Y. (2006). *Angew. Chem. Int. Ed.* **45**, 3740–3747.
Cherian, M. & Abraham, E. C. (1995). *Biochem. Biophys. Res. Commun.* **208**, 675–679.
Connon, S. J. & Blechert, S. (2003). *Angew. Chem. Int. Ed.* **42**, 1900–1923.
Coppens, P., Novozhilova, I. & Kovalevsky, A. Y. (2002). *Chem. Rev.* **102**, 861–883.
DeBeer George, S., Huang, K. W., Waymouth, R. M. & Solomon, E. I. (2006). *Inorg. Chem.* **45**, 4468–4477.
Delgado-Jaime, M. U., Conrad, J. C., Fogg, D. E. & Kennepohl, P. (2006). *Inorg. Chim. Acta*, **359**, 3042–3047.
Dey, A., Jenney, F. E., Adams, M. W. W., Johnson, M. K., Hodgson, K. O., Hedman, B. & Solomon, E. I. (2007). *J. Am. Chem. Soc.* **129**, 12418–12431.
Fomitchev, D. V., Bagley, K. A. & Coppens, P. (2000). *J. Am. Chem. Soc.* **122**, 532–533.
Frank, P., DeBeer George, S., Anxolabehere-Mallart, E., Hedman, B. & Hodgson, K. O. (2006). *Inorg. Chem.* **45**, 9864–9876.
Furstner, A. (2000). *Angew. Chem. Int. Ed.* **39**, 3013–3043.
Getty, K., Delgado-Jaime, M. U. & Kennepohl, P. (2007). *J. Am. Chem. Soc.* **129**, 15774–15776.
Getty, K., Delgado-Jaime, M. U. & Kennepohl, P. (2008). *Inorg. Chim. Acta*, **361**, 1059–1065.
Glaser, C. B., Yamin, G., Uversky, V. N. & Fink, A. L. (2005). *Biochim. Biophys. Acta Prot. Proteom.* **1703**, 157–169.
Grubbs, R. H. (2004). *Tetrahedron*, **60**, 7117–7140.
Grubbs, R. H. (2006). *Angew. Chem. Int. Ed.* **45**, 3760–3765.
Hong, S. H., Day, M. W. & Grubbs, R. H. (2004). *J. Am. Chem. Soc.* **126**, 7414–7415.
Hortala, M. A., Fabbrizzi, L., Foti, F., Licchelli, M., Poggi, A. & Zema, M. (2003). *Inorg. Chem.* **42**, 664–666.
Imlau, M., Haussiihl, S., Woike, T., Schieder, R., Angelov, V., Rupp, R. A. & Schwarz, K. (1999). *Appl. Phys. B*, **68**, 877–885.
Imlau, M., Woike, T., Schieder, R. & Rupp, R. A. (1999). *Phys. Rev. Lett.* **82**, 2860–2863.
Jacob, C., Giles, G. L., Giles, N. M. & Sies, H. (2003). *Angew. Chem. Int. Ed.* **42**, 4742–4758.
Kadlcik, V., Sicard-Roselli, C., Houee-Levin, C., Kodicek, M., Ferreri, C. & Chatgilialoglu, C. (2006). *Angew. Chem. Int. Ed.* **45**, 2595–2598.

Karunakaran-Datt, A. & Kennepohl, P. (2009). *J. Am. Chem. Soc.* **131**, 3577–3582.
Kishita, A., Nishino, S., Togashi, T. & Nishida, Y. (2005). *Synth. React. Inorg. Met. Org. Nano-Metal Chem.* **35**, 677–681.
Kunkely, H. & Vogler, A. (2001). *Inorg. Chim. Acta*, **325**, 179–181.
Lam, X. M., Yang, J. Y. & Cleland, J. L. (1997). *J. Pharm. Sci.* **86**, 1250–1255.
Leung, B. O., Jalilehvand, F. & Szilagyi, R. K. (2008). *J. Phys. Chem. B*, **112**, 4770–4778.
Martin-Diaconescu, V. & Kennepohl, P. (2007). *J. Am. Chem. Soc.* **129**, 3034–3035.
Nicolaou, K. C., Bulger, P. G. & Sarlah, D. (2005). *Angew. Chem. Int. Ed.* **44**, 4490–4527.
Pickering, I. J., Prince, R. C., Divers, T. & George, G. N. (1998). *FEBS Lett.* **441**, 11–14.
Rachford, A. A., Peterson, J. L. & Rack, J. J. (2005). *Inorg. Chem.* **44**, 8065–8075.
Rachford, A. A., Peterson, J. L. & Rack, J. J. (2006). *Inorg. Chem.* **45**, 5953–5960.
Rachford, A. A., Peterson, J. L. & Rack, J. J. (2007). *Dalton Trans.* pp. 3245–3251.
Rachford, A. A. & Rack, J. J. (2006). *J. Am. Chem. Soc.* **128**, 14318–14324.
Rack, J. J. & Mockus, N. V. (2003). *Inorg. Chem.* **42**, 5792–5794.
Rack, J. J., Rachford, A. A. & Shelker, A. M. (2003). *Inorg. Chem.* **42**, 7357–7359.
Ray, K., DeBeer George, S., Solomon, E. I., Wieghardt, K. & Neese, F. (2007). *Chem. Eur. J.* **13**, 2783–2797.
Requena, J. R., Dimitrova, M. N., Legname, G., Teijeira, S., Prusiner, S. B. & Levine, R. L. (2004). *Arch. Biochem. Biophys.* **432**, 188–195.
Schrock, R. R. (2006). *Angew. Chem. Int. Ed.* **45**, 3748–3759.
Tenderholt, A. L., Szilagyi, R. K., Holm, R. H., Hodgson, K. O., Hedman, B. & Solomon, E. I. (2008). *Inorg. Chem.* **47**, 6382–6392.